World Academy of Science, Engineering and Technology
International Journal of Mechanical and Mechatronics Engineering
Vol:6, No:11, 2012

FEA for Transient Responses of an S-Shaped Force Transducer with a Viscoelastic Absorber Using a Nonlinear Complex Spring

T. Yamaguchi, Y. Fujii, A. Takita and T. Kanai

***Abstract*—**To compute dynamic characteristics of nonlinear viscoelastic springs with elastic structures having huge degree-of-freedom, Yamaguchi proposed a new fast numerical method using finite element method [1]-[2]. In this method, restoring forces of the springs are expressed using power series of their elongation. In the expression, nonlinear hysteresis damping is introduced. In this expression, nonlinear complex spring constants are introduced. Finite element for the nonlinear spring having complex coefficients is expressed and is connected to the elastic structures modeled by linear solid finite element. Further, to save computational time, the discrete equations in physical coordinate are transformed into the nonlinear ordinary coupled equations using normal coordinate corresponding to linear natural modes. In this report, the proposed method is applied to simulation for impact responses of a viscoelastic shock absorber with an elastic structure (an S-shaped structure) by colliding with a concentrated mass. The concentrated mass has initial velocities and collides with the shock absorber. Accelerations of the elastic structure and the concentrated mass are measured using Levitation Mass Method proposed by Fujii [3]. The calculated accelerations from the proposed FEM, corresponds to the experimental ones. Moreover, using this method, we also investigate dynamic errors of the S-shaped force transducer due to elastic mode in the S-shaped structure.

***Keywords*—**Transient response, Finite Element analysis, Numerical analysis. Viscoelastic shock absorber, Force transducer.

I. Introduction

TO reduce impacts from precision instruments and so on, viscoelastic shock absorbers are used. These viscoelastic absorbers sometimes have nonlinearity between their restoring forces and deformations under relatively large load. Moreover, their restoring forces sometimes have nonlinearity in hysteresis. Therefore, it is of importance to clarify nonlinear dynamic properties of viscoelastic absorbers with elastic structures under impact load.

This paper deals with numerical analysis of impact responses for a viscoelastic shock absorber connected with an elastic structure (an S-shaped structure) using a fast finite element method proposed by Yamaguchi [1]-[2]. In this analysis, the viscoelastic absorber is modeled by using a nonlinear complex spring. The restoring force of the spring is expressed as power series of its elongation. The restoring force also includes nonlinear hysteresis damping. Therefore, complex spring constants are introduced for not only the linear component but also nonlinear components of the restoring force. Finite element for the nonlinear complex spring is expressed and is connected to an elastic structure modeled by linear solid finite elements.

The discrete equations of this system in physical coordinate are transformed into the nonlinear ordinary coupled equations using normal coordinate corresponding to linear natural modes. The transformed equations are integrated numerically in extremely small degree-of-freedom.

In this paper, we apply our proposed FEM to examine dynamic errors in an S-shaped force transducer when transient responses of a viscoelastic shock absorber are measured. The transient responses are obtained when a concentrated mass (i.e. a rigid levitated block) is collided with the absorber. The elastic structure in this study is an S-shaped structure, which is a part of the force transducer as shown in Fig.1.

To investigate the dynamic errors in the transducer, the reference force is measured using Levitation Mass Method proposed by Fujii [3]. The experimental dynamic errors [3] are compared with the calculated ones from our proposed FEM.

II. Experimental System [3]

Fig. 1 shows the outline of the experimental system carried out by Fujii [3]. To evaluate mechanical responses of a viscoelastic shock absorber, an S-shaped force transducer is connected with the absorber. A mass levitated by linear pneumatic bearing is collided with the absorber in *y* direction, and transient responses are measured using the force transducer. The S-shaped structure in the force transducer has two thin portions as twin beams near the central hole as shown in Fig.2. These two beams play a role of a pair of parallel springs in *y* direction. When external load is applied in *y* direction, strains are measured using strain gauges fabricated in the S-shaped structure. Using the strains, forces F_{trans} of the transient responses are measured.

To verify precision of the measured force F_{trans}, Fujii also measured the velocity v_1 of the levitated mass using an interferometer as shown in Fig.1. By differentiating the measured velocity v_1, acceleration a_1 of the levitated mass is obtained. Further, the reference force $F_{mass} = M_1 a_1$ is identified

T. Yamaguchi is with the Mechanical System Engineering Department, Gunma University, Kiryu, Japan (e-mail: yamagme3@gunma-u.ac.jp).
Y. Fujii is with the Electronic Engineering Department, Gunma University, Kiryu, Japan.
ATakita is with the Electronic Engineering Department, Gunma University , Kiryu, Japan.
T. Kanai is with the Graduate School of the Mechanical System Engineering Department, Gunma University , Kiryu, Japan .

using the acceleration a_1 and mass $M_1 = 2.6526kg$ of the levitated mass. Fujii compared between the reference force

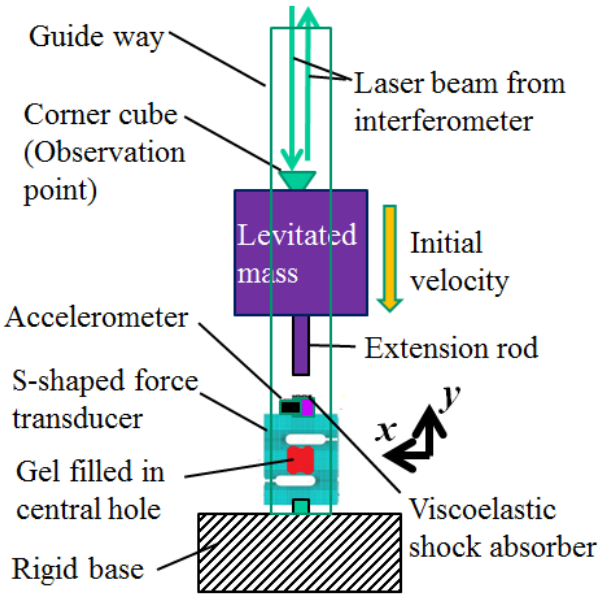

Fig. 1 Outline of experimental system [3]

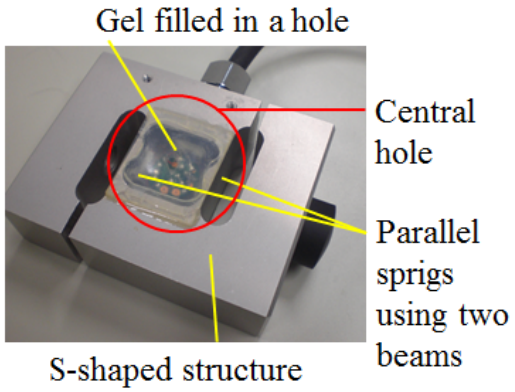

Fig. 2 Photo of the S-shaped force transducer [3]

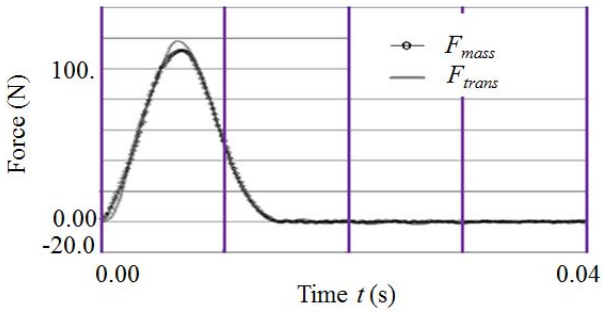

Fig. 3 Comparison between the measured force F_{trans} from the S-shaped transducer and the reference force F_{trans} using Levitation Mass Method [3]

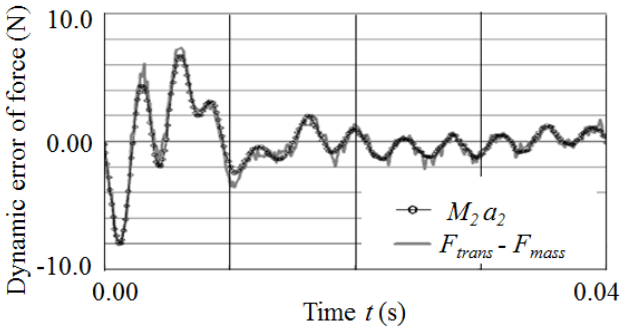

Fig. 4 Comparison between the measured dynamic error $\Delta F = F_{trans} - F_{mass}$ and the estimated error using acceleration $M_2 a_2$ of the S-shaped structure [3]

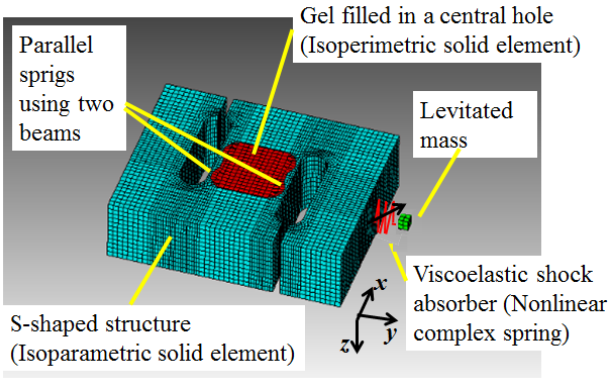

Fig. 5 Simulation model of the viscoelastic shock absorber and the S-shaped force transducer [3]

F_{mass} and the force F_{trans} obtained from the S-shaped transducer as shown in Fig.3. And he showed that there exist small dynamic errors in the measured force F_{trans} of the S-shaped force transducer. Fig.4 shows a time history of the discrepancy $\Delta F = F_{trans} - F_{mass}$ between the measured force F_{trans} by the transducer and the reference force F_{mass}. Further, Fujii found out that the discrepancy $\Delta F = F_{trans} - F_{mass}$ corresponds to the force calculated by $M_2 a_2$. a_2 is the acceleration of the S-shaped structure and M_2 is the half of the mass for the S-shaped structure. Using $\Delta F \cong M_2 a_2$, Fujii proposed a correction method of the measured force F_{trans}. To obtain correction force ΔF, he added an accelerometer to the S-shaped structure as shown Fig.1. The measured acceleration a_2 is utilized to correct the measured force F_{trans} in real time.

In this paper, to investigate the correction force ΔF (i.e. the discrepancy between F_{trans} and F_{mass}) in detail, numerical simulations for this experimental system are performed.

We also use the experimental results to verify our proposed numerical method using FEA (i.e. Finite Element Analysis) with a nonlinear complex spring.

The detail conditions of this experimental system are added as follows. The experimental system has the levitated mass (i.e.

a levitated rigid block), which can smoothly travel along a guide way in y direction due to a pneumatic linear bearing as shown in Fig.1. The block is levitated due to air film (thickness is 8 (μm)) at the interfaces between the block and the guide. Pressure at the interfaces is self-controlled by orifice effect to maintain the thickness of the air film. Owing to this system, the block can move toward the y-direction under extremely low friction. An extension rod is connected with the levitated mass. These parts have a role of moving parts with initial velocity v_0 given by a hand. The moving parts collide with the small strip of the viscoelastic shock absorber attached with one end of the S-shaped structure. This experimental system is proposed and named as Levitation Mass method by Fujii [4]-[6]. In the vicinity of this end of the transducer, the accelerometer is fabricated. Another end of the transducer is fixed on the rigid base. A gel is filled in the central hole of the S-shaped structure to obtain damping effect as shown in Fig.2.

III. Numerical Procedure

Fig. 5 represents the FEM model for the S-shaped structure in the force transducer to evaluate. In this figure, the S-shaped structure is modeled as an elastic body using finite elements, and the levitated mass is modeled by a concentrated mass. The viscoelastic shock absorber is modeled by a nonlinear spring with nonlinear damping. Origin of this model is set on the position where the levitated mass begins to contact with the viscoelastic absorber. An initial velocity v_0 = -180 (mm/sec) in y-direction is given to the concentrated mass (i.e. the levitated mass).

A. Discretized Equation for the Viscoelastic Absorber

A small strip of the viscoelastic absorber is modeled by using a concentrated nonlinear spring with nonlinear hysteresis. To represent the nonlinear hysteresis, we propose to introduce a nonlinear complex spring. As shown in Fig.5, it is assumed that the nonlinear complex spring with viscoelasticity has principal elastic axis in y direction. We denote displacement as $U_{\alpha y}$ in y direction at the nodal point α where one end of the nonlinear complex spring (i.e. the viscoelastic absorber) is connected with the S-shaped force transducer. $U_{\beta y}$ is the displacement at the nodal point β on another end of the nonlinear complex spring. The levitated block is connected at the nodal point β. Nonlinear function using power series is given for the nodal force of the spring at the point α. Therefore, restoring force of the spring is expressed as $R_{\alpha y} = \gamma_1(U_{\alpha y}-U_{\beta y}) + \gamma_2(U_{\alpha y}-U_{\beta y})^2 + \gamma_3(U_{\alpha y}-U_{\beta y})^3$ using the relative displacement $U_{\alpha y}$ - $U_{\beta y}$ between $U_{\alpha y}$ and $U_{\beta y}$. Further, linear hysteresis damping is introduced as $\gamma_1 = \bar{\gamma}_1(1+j\eta_{s1})$. $\bar{\gamma}_1$ is the real part of γ_1, and η_{s1} is material loss factor of the concentrated spring. j is imaginary unit. Moreover, nonlinear hysteresis damping is also introduced as $\gamma_2 = \bar{\gamma}_2(1+j\eta_{s2})$, $\gamma_3 = \bar{\gamma}_3(1+j\eta_{s3})$ in the same manner. $\bar{\gamma}_2$ and $\bar{\gamma}_3$ are the real part of γ_2 and γ_3 ,respectively. η_{s2} and η_{s3} are nonlinear components of material loss factor for the concentrated spring, respectively. For the nonlinear complex spring, nonlinear spring constants have complex quantity to represent changes of hysteresis due to the deformation of the spring. These relations can be rewritten in the matrix form as:

$$\{r\} = [\gamma_1]\{U_s\} + \{\bar{d}\},$$

$$[\gamma_1] = \begin{bmatrix} 0 & 0 & 0 & 0 & 0 & 0 \\ 0 & \gamma_1 & 0 & 0 & -\gamma_1 & 0 \\ 0 & 0 & 0 & 0 & 0 & 0 \\ 0 & 0 & 0 & 0 & 0 & 0 \\ 0 & -\gamma_1 & 0 & 0 & \gamma_1 & 0 \\ 0 & 0 & 0 & 0 & 0 & 0 \end{bmatrix},$$

$$\{\bar{d}\} = \begin{Bmatrix} 0 \\ +\gamma_2(U_{\alpha y}-U_{\beta y})^2 + \gamma_3(U_{\alpha y}-U_{\beta y})^3 \\ 0 \\ 0 \\ -\gamma_2(U_{\alpha y}-U_{\beta y})^2 - \gamma_3(U_{\alpha y}-U_{\beta y})^3 \\ 0 \end{Bmatrix} \quad (1)$$

where $\{r\} = \{0, R_{\alpha y}, 0, 0, R_{\beta y}, 0\}^T$ is nodal force vector at the nodes α and β. $\{U_s\} = \{U_{\alpha x}, U_{\alpha y}, U_{\alpha z}, U_{\beta x}, U_{\beta y}, U_{\beta z}\}^T$ is nodal displacement vector at the nodes. $[\gamma_1]$ is complex stiffness matrix involving only linear term of the restoring force. $\{\bar{d}\}$ is vector containing nonlinear terms of the restoring force.

For the later computations, we use nonlinear complex spring constants as $\bar{\gamma}_1$=1.37$\times$ 10^4 (N/m), $\bar{\gamma}_2$=0.00 (N/m^2), $\bar{\gamma}_3$=2. 35 $\times 10^{11}$ (N/m^3), η_{s1}=0.300, η_{s2}=0.000, η_{s3}=0.300.

B. Discretized Equations of the S-Shaped Force Transducer Filled with the Gel

We assumed that equations of motion for the elastic structure of the S-shaped force transducer are expressed under infinitesimal deformation using a conventional three dimensional finite element method. To add damping effects, a viscoelastic gel is filled in the central hole of the force transducer as shown in Fig.2. Thus, we also create the three dimensional finite elements for the gel as depicted in Fig.5. Viscoelasticity of the gel is taken into account using complex modulus of elasticity $\bar{E}_g = E_g(1+j\eta_g)$. The real part E_g of the $\bar{E}_g$ stands for storage modulus of elasticity while η_g is material loss factor of the gel. For the transducer made by aluminum, complex modulus of elasticity $\bar{E}_f = E_f(1+j\eta_f)$ is also considered. By superposing all elements related to the S-shaped transducer and the gel, the following equations are obtained.

$$[M_s]\{\ddot{u}_s\} + [K_s]\{u_s\} = \{f_s\} \quad (2)$$

where, $[M_s]$, $[K_s]$, $\{f_s\}$ and $\{u_s\}$ are mass matrix, complex stiffness matrix, nodal force vector and displacement vector for the S-shaped transducer and the gel, respectively. Isoparametric hexahedral elements with non- conforming modes are mainly used for the three dimensional finite elements.

C. Discrete Equation for Combined System between the S-Shaped Force Transducer with the Gel and the Viscoelastic Absorber with the Levitated Block

The restoring force $\{r\}$ in Eq. (1) is added to the nodal force at the ends of the nonlinear complex spring on the nodes α and β. On the node α, the nonlinear complex spring (i.e. the viscoelastic absorber) is connected with the S-shaped force transducer. On the node β, the spring is attached with the levitated mass modeled as a concentrated mass. And then the following expression in global system can be obtained:

$$[M]\{\ddot{u}\}+[K]\{u\}+\{\hat{d}\}=\{f\} \tag{3}$$

where, $\{u\}$, $[M]$, $[K]$ and $\{f\}$ are displacement vector, mass matrix, complex stiffness matrix and external force vector in global system, respectively. $\{\hat{d}\}$ is modified from $\{\bar{d}\}$ to have the identical vector size to degree- of- freedom of the Eq.(3).

D. Approximate Computation of Modal Damping

To calculate linear modal damping (i.e. modal loss factor), we consider the following complex eigenvalue problem by neglecting the terms of the non-linear restoring force and the external force.

$$\sum_{e=1}^{e\max}(-(\omega^{(i)})^2(1+j\eta_{tot}^{(i)})[M]_e+[K_R]_e(1+j\eta_e))\{\phi^{(i)}\}=\{0\} \tag{4}$$

In this equation, superscript (i) stands for the i-th eigenmode. η_e includes η_{s1}, η_f and η_g. $(\omega^{(i)})^2$ is the real part of complex eigenvalue. $\{\phi^{(i)}\}$ is the complex eigenvector and $\eta_{tot}^{(i)}$ is the modal loss factor. Next, we introduce the following β_e using the maximum value $\eta_{\max}$ among the elements' material loss factors η_e, $(e=1,2,3,..e_{\max})$.

$$\beta_e=\eta_e/\eta_{\max},\ \beta_e\le 1 \tag{5}$$

On assumption of $\eta_{\max}<<1$, solutions of Eq.(4) are expanded using a small parameter $\mu=j\eta_{\max}$:

$$\{\phi^{(i)}\}=\{\phi^{(i)}\}_0+\mu\{\phi^{(i)}\}_1+\mu^2\{\phi^{(i)}\}_2+,... \tag{6}$$

$$(\omega^{(i)})^2=(\omega_0^{(i)})^2+\mu^2(\omega_2^{(i)})^2+\mu^4(\omega_4^{(i)})^2+,... \tag{7}$$

$$j\eta_{tot}^{(i)}=\mu\eta_1^{(i)}+\mu^3\eta_3^{(i)}+\mu^5\eta_5^{(i)}+\mu^7\eta_7^{(i)}+,... \tag{8}$$

In these equations, under conditions of $\beta_e\le 1$ and $\eta_{\max}<<1$, we can obtain $\eta_{\max}\beta_e<<1$. Thus, $\mu\beta_e$ is regarded as small parameters like μ

In the equations, $\{\phi^{(i)}\}_0$, $\{\phi^{(i)}\}_1$, $\{\phi^{(i)}\}_2$,... and $(\omega_0^{(i)})^2$, $(\omega_2^{(i)})^2$, $(\omega_4^{(i)})^2$,... and $\eta_1^{(i)}$, $\eta_3^{(i)}$, $\eta_5^{(i)}$,... have real quantities. Substituting Eqs.(6)-(8) into Eq. (4) yields approximate equations using μ^0 and μ^1 orders. The following equation can be derived by arranging the approximate equations:

$$\eta_{tot}^{(i)}=\sum_{e=1}^{e\max}\left(\eta_e S_e^{(i)}\right), \tag{9}$$

$$S_e^{(i)}=\{\phi^{(i)}\}_0^T[K_R]_e\{\phi^{(i)}\}_0/\sum_{e=1}^{e\max}\left(\{\phi^{(i)}\}_0^T[K_R]_e\{\phi^{(i)}\}_0\right)$$

According to these expressions, modal loss factor $\eta_{tot}^{(i)}$ can be calculated using material loss factors η_e of each element e, share $S_e^{(i)}$ of strain energy of each element to total strain energy. The parameter $\eta_e S_e^{(i)}$ corresponds to damping contribution of each element e to the entire system.

E. Conversion from the Discretized Equation in Physical Coordinate to the Nonlinear Equation in Normal Coordinate

It takes huge amount of computational time to calculate Eq.(3) in physical coordinate, directly. In this section, a numerical manipulation is proposed to decrease the degree-of-freedom for the discretized equations of motion.

First, we assume that linear natural modes $\{\phi^{(i)}\}$ of vibration can be approximated to $\{\phi^{(i)}\}_0$. Next, by introducing normal coordinates $\tilde{b}_i$ corresponding to the linear natural modes $\{\phi^{(i)}\}_0$, the nodal displacement vector can be expressed using both $\{\phi^{(i)}\}_0$ and $\tilde{b}_i$ as follows.

$$\{u\}=\sum_i \tilde{b}_i\{\phi^{(i)}\}_0 \tag{10}$$

By substitution of Eq.(10) into Eq.(3), the following nonlinear ordinary simultaneous equations as to normal coordinates $\tilde{b}_i$ can be obtained as:

$$\tilde{b}_{i,tt}+\eta_{tot}{}^{(i)}\omega_0{}^{(i)}\tilde{b}_{i,t}+(\omega_0{}^{(i)})^2\tilde{b}_i+\sum_j\sum_k \tilde{D}_{ijk}\tilde{b}_j\tilde{b}_k+\sum_j\sum_k\sum_l \tilde{E}_{ijkl}\tilde{b}_j\tilde{b}_k\tilde{b}_l$$
$$=\tilde{P}_i,\ (i,j,k,l=1,2,3,...) \tag{11}$$
$$\tilde{D}_{ijk}=\gamma_2(\phi_{\alpha iy}-\phi_{\beta iy})(\phi_{\alpha jy}-\phi_{\beta jy})(\phi_{\alpha ky}-\phi_{\beta ky}),$$
$$\tilde{E}_{ijkl}=\gamma_3(\phi_{\alpha iy}-\phi_{\beta iy})(\phi_{\alpha jy}-\phi_{\beta jy})(\phi_{\alpha ky}-\phi_{\beta ky})(\phi_{\alpha ly}-\phi_{\beta ly}),$$
$$\tilde{P}_i=\{\phi^{(i)}\}_0{}^T\{f\}$$
$$\{\phi^{(i)}\}_0=\{\phi_{1ix},\phi_{1iy},\phi_{1iz},\phi_{2ix},\phi_{2iy},\phi_{2iz},\phi_{3ix},...\}^T$$

In Eq.(11), $\omega_0{}^{(i)}$ represents the i-th natural frequency. $\eta_{tot}{}^{(i)}$ is the i-th modal loss factor. Since Eq.(11) has much smaller degree-of-freedom than that of Eq.(3), we can save computational time drastically. In Eq.(11), subscript t following a comma stands for partial differentiation with respect to time t. $\phi_{\alpha iy}$ is the y-component of the eigenmode $\{\phi^{(i)}\}_0$ at the connected node α between the S-shaped force transducer and the viscoelastic shock absorber.

F. Nonlinear Impact Response

We give an initial velocity to the levitated mass connected with the viscoelastic shock absorber. And nonlinear impact responses of the S-shaped force transducer with the viscoelastic absorber are calculated by applying Runge-Kutta-Gill method to Eq.(11).

IV. Numerical Results and Discussion

A. Verification of the Proposed Numerical Method

First, we verify our proposed numerical method using Finite Element Analysis with nonlinear complex spring. Fig.6 shows time histories of the measured and calculated reference forces F_{mass} using the levitated mass. These reference forces are obtained by $F_{mass} = M_1 a_1$, where a_1 is the measured or calculated acceleration. In this graph, the origin of time is set when the levitated mass begins to collide with the viscoelastic shock absorber connected with the S-shaped structure. From Fig.6, the calculated reference force is consistent with the measured one. We can say that the reference force can be simulated using our proposed FEA for the transient response of the viscoelastic shock absorber.

Next, we compute dynamic errors of the S-shaped force transducer. Fujii found out in the previous paper [3] that the dynamic errors ΔF of the transducer have relationship as $\Delta F \cong M_2 a_2$. a_2 is the measured acceleration from the accelerometer fabricated on the S-shaped structure. And M_2 is

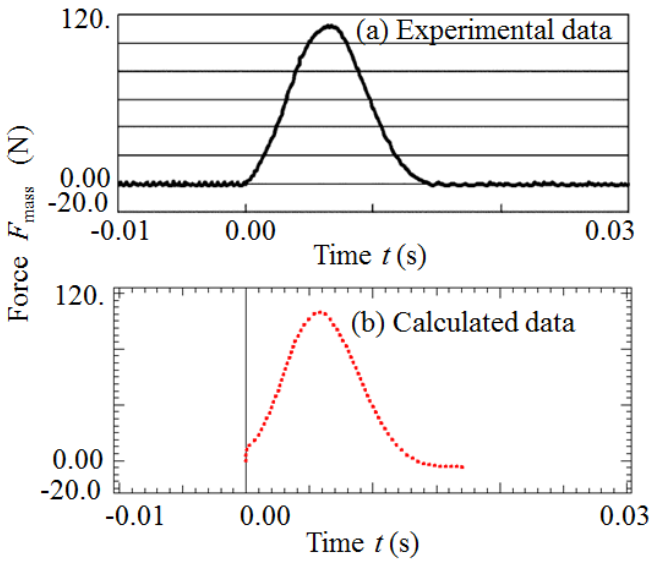

Fig. 6 Comparison of the reference force using the levitated mass between calculated data and measured data [3]

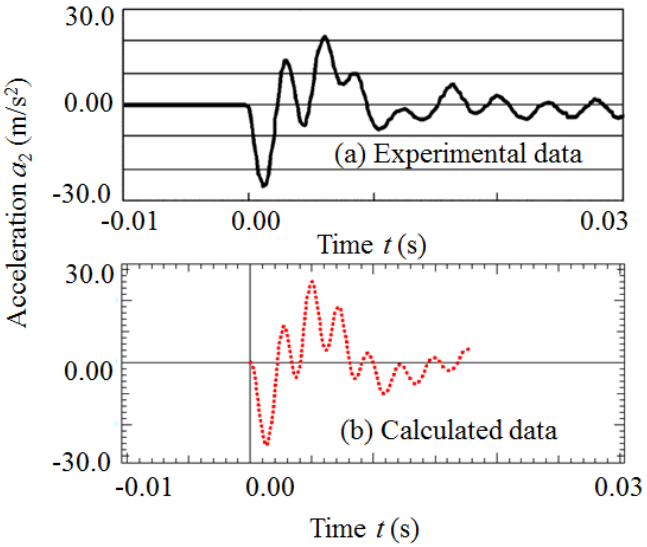

Fig. 7 Comparison o f the acceleration at the S-shaped structure between calculated data and measured data [3]

the half of the mass for the S-shaped structure. Therefore, to investigate the dynamic errors, we simulate the acceleration a_2 on the S-shaped structure.

Fig. 7 (b) shows the calculated time history of the acceleration a_2 for the S-shaped structure in comparison with an experimental one in Fig.7 (a). As illustrated in Fig. 8:

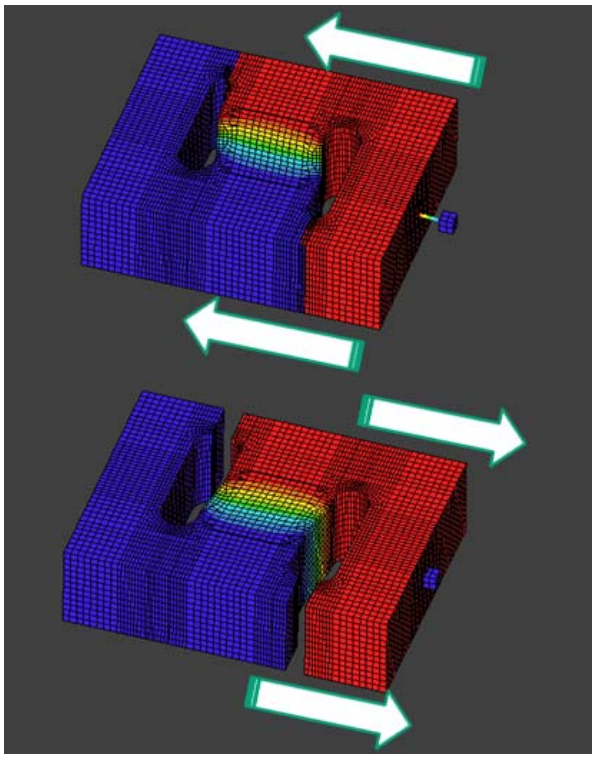

Fig. 8 Elastic mode of the S-shaped structure in y-direction appeared in dynamic errors of the transducer

The calculated curve in Fig.7 (b) using nonlinear complex spring for the viscoelastic shock absorber is consistent with experimental data in Fig.7 (a). In Fig. 7, we can find two typical periods both in the experimental and calculated accelerations at the S-shaped structure. The short period 0.0025(S) corresponds to the eigen frequency of the elastic mode for the S-shaped structure in *y*-direction as shown in Fig.8.

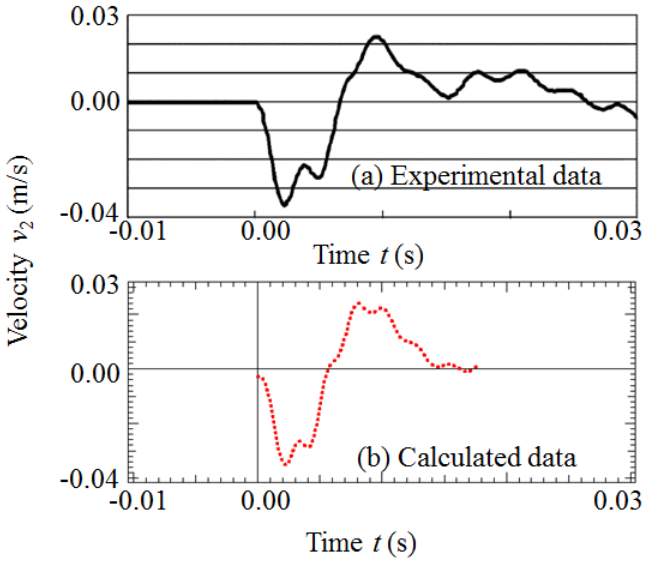

Fig. 9 Comparison of the velocity at the S-shaped structure between calculated data and measured data [3]

As can be seen this figure, a half part of the S-shaped structure moves in this eigenmode, while the other half part of the S-shaped structure is at rest. Therefore, in this mode, the dynamic motion of the half part for the S-shaped structure is dominant. This fact leads that the correction method proposed by Fujii [3] using the acceleration a_2 and the half mass M_2 of the S-shaped structure is proper.

The long period 0.013 (s) is related with the subharmonic component of order 1/7 for this elastic mode. Moreover, the long period is also related with the superharmonic component of order seven for the translation mode of the concentrated mass (i.e. the levitated mass) in y-direction. These relations can be regarded as internal resonance. This is caused by the nonlinearity of the viscoelastic shock absorber.

Additionally, Fig.9 shows the measured and calculated velocities at the S-shaped structure. Both results also agree well.

B. Effect of Material Properties for Gel on Dynamic Errors of S-Shaped Force Transducer

Next, we investigate influences of the material properties of the gel filled in the central hole on the dynamic errors of the S-shaped structure. For the previous simulations in Figs. 6-9, we use the material loss factor η_g =0.700 (-) and the storage modulus of elasticity E_g =0.00400 (GPa) for the gel. Under this condition, we obtain the modal loss factor $\eta_{tot}^{(i)}$ =0.0496 (-) for the dominant eigen mode on the dynamic errors (i.e. the elastic mode of the S-shaped structure in *y*-direction) as shown in Fig.8. According to Eq. (9), to increase modal damping $\eta_{tot}^{(i)}$ using the gel, we have to increase not only the material loss factor η_g of the gel but also the share of the strain energy of the gel to the total strain energy in this system.

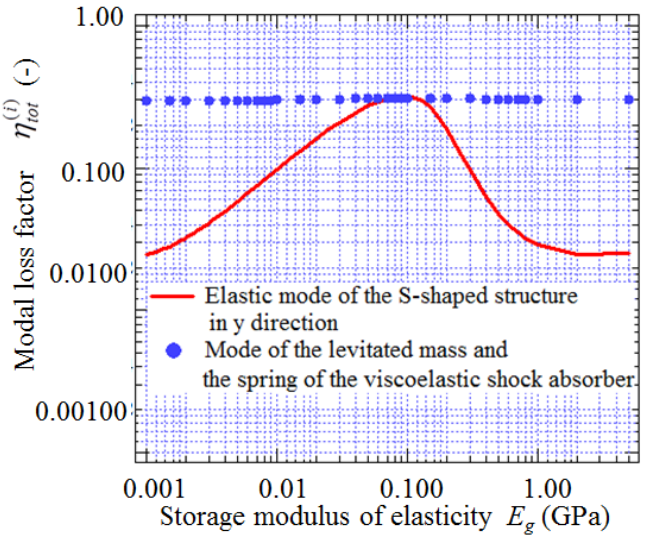

Fig. 10 Effects of elasticity E_g of the gel on modal loss factors $\eta_{tot}^{(i)}$

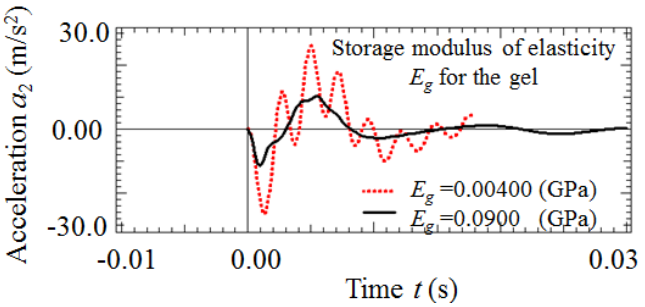

Fig. 11 Effects of elasticity E_g of the gel on dynamic errors of the force transducer

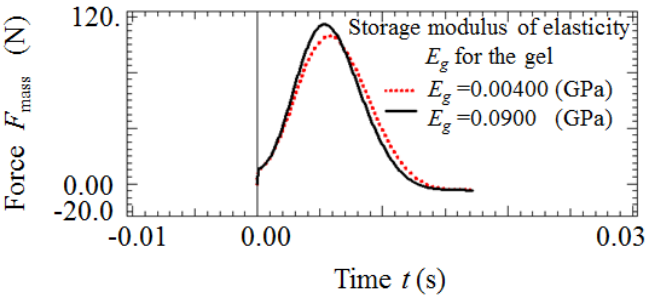

Fig. 12 Effects of elasticity E_g of the gel on the reference force

Fig.10 shows the relation between the modal loss factors $\eta_{tot}^{(i)}$ in this system and the storage modulus of elasticity E_g for the gel. In this graph, the constant value η_g =0.700 (-) is given for the material loss factor of the gel. Thus, the change of the modal loss factor $\eta_{tot}^{(i)}$ in Fig.10 is caused by the change of the share of

the strain energy in the gel. As shown in Fig.10, the modal loss factor $\eta_{tot}^{(i)}$ has the local maximum value $\eta_{tot}^{(i)}$=0.318 (-) near E_g =0.0900 (GPa). Using the local maximum value, we compute a time history of the acceleration a_2 for the S-shaped structure as shown in Fig.11. The component of the short period for the mode decreases due to the increment of $\eta_{tot}^{(i)}$. This leads to less dynamic errors ΔF in the measured force using the force transducer. Fig.12 shows changes of the reference forces F_{mass} due to change of the modal loss factor from the initial value $\eta_{tot}^{(i)}$ =0.0496 (-) to the local maximum value $\eta_{tot}^{(i)}$=0.318 (-). There exist significant changes of the reference force F_{mass} due to the increase of the storage modulus of elasticity E_g for the gel. Therefore, the measured force using the force transducer is affected if we give too large storage modulus of elasticity E_g for the gel. Thus, this result reveals that it is undesirable to use too large storage modulus of elasticity E_g for precision measurement of the force, even though we obtain less dynamic errors due to the elastic mode in the S-shaped transducer.

Fig.13 shows time histories of the reference force F_{mass} when the storage modulus of elasticity E_g changes from E_g =0.00 100 (GPa) to 0.00900 (GPa). These values of E_g are less than the maximal value E_g =0.0900 (GPa) in Fig.12. The corresponding modal loss factor $\eta_{tot}^{(i)}$ changes from $\eta_{tot}^{(i)}$ =0.0277 (-) to $\eta_{tot}^{(i)}$=0.0928 (-) as E_g increases. As shown in Fig.13, the curves of the reference force F_{mass} never change under this condition. From these results, there are no influences on the reference force when the storage modulus of elasticity for the gel is less than 0.00900 (GPa). Using the same conditions for the storage modulus of elasticity E_g, we also compute the time histories of acceleration a_2 for the S-shaped structure as shown in Fig.14. The acceleration a_2 decreases as E_g increases from E_g =0.00100 (GPa) to 0.00900 (GPa). From these results, it is possible to reduce the dynamic errors due to the acceleration a_2 of the S-shaped structure without influences on the

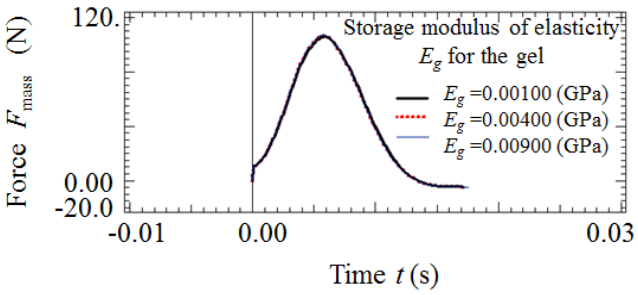

Fig. 13 Effects of elasticity E_g of the gel on the reference force F_{mass}

reference force F_{mass}, when we set the storage modulus of elasticity E_g =0.00900 (GPa) for the gel.

On the other hand, the modal loss factors $\eta_{tot}^{(i)}$ are also written in Fig.10 for the mode related with the long period in the dynamic errors in Fig.7. As shown in Fig.10, $\eta_{tot}^{(i)}$ for this mode (i.e. the mode of the levitated mass and the spring of the absorber) maintains a constant value, though the storage modulus of elasticity changes. The constant value corresponds to the material loss factor η_{s1} =0.300 for the viscoelastic shock absorber. Thus, there are small influences of storage modulus of elasticity E_g on these modal loss factors $\eta_{tot}^{(i)}$ for this mode. This implies that effects of the gel are small on the component of the long period in dynamic errors.

According to Eq. (9), the modal loss factor $\eta_{tot}^{(i)}$ also increases as the material loss factor η_g of the gel increases.

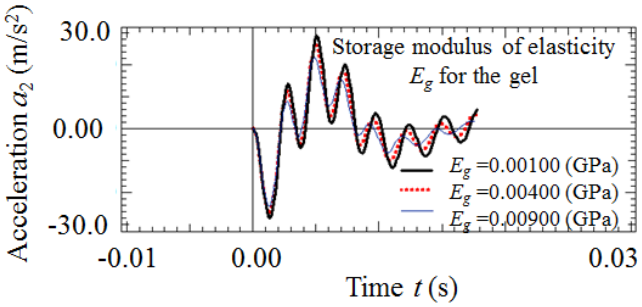

Fig. 14 Effects of elasticity E_g of the gel on dynamic errors of the force transducer

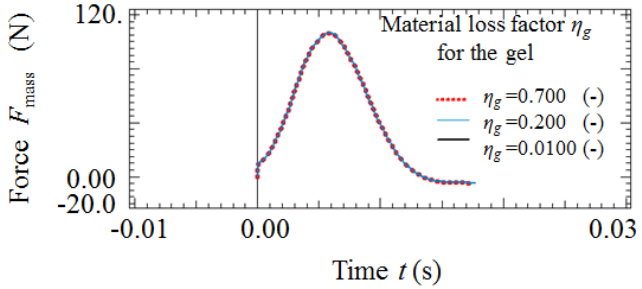

Fig. 15 Effects of material loss factor η_g of the gel on the reference force F_{mass}

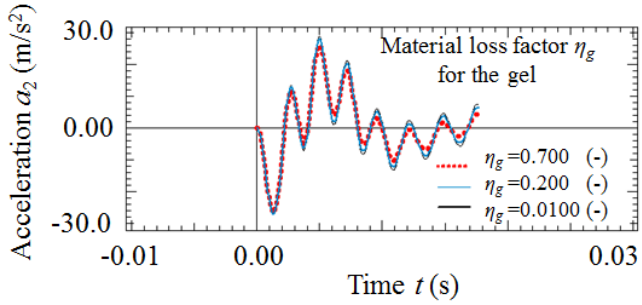

Fig. 16 Effects of material loss factor η_g of the gel on dynamic errors of the force transducer

When the material loss factor η_g of the gel changes from η_g =0.0100 (-) to η_g =0.700 (-) under the constant storage modulus of elasticity E_g =0.00400 (GPa), Figs.15 and 16 show the calculated reference force F_{mass} and the calculated acceleration a_2 of the S-shaped structure (i.e. dynamic error), respectively. The corresponding modal loss factor $\eta_{tot}^{(i)}$ changes from $\eta_{tot}^{(i)}$ =0.0144 (-) to $\eta_{tot}^{(i)}$ =0.0496 (-). As shown in Fig.16, the dynamic error decreases as the material loss factor η_g of the gel increases. On the other hand, the reference force F_{mass} does not change though the material loss factor η_g of the gel increases as shown in Fig.15. These results imply that the material loss factor η_g of the gel can reduce the dynamic error of the force transducer without the influences on the reference force F_{mass} .

V. Conclusion

By applying the numerical method proposed by Yamaguchi, simulation was carried out for impact responses of a viscoelastic shock absorber with an S-shaped elastic structure. This fast computational method using nonlinear finite element method is aimed for nonlinear impact responses of elastic structures connected with nonlinear concentrated springs with nonlinear hysteresis.

The restoring force of the spring is assumed to express as power series of elongation with nonlinear hysteresis damping. In this expression, nonlinear complex spring constants are introduced. Finite element for the nonlinear complex spring is expressed and is connected to elastic structures modeled by linear solid finite elements. Further, the discretized equations in physical coordinate are transformed into the nonlinear ordinary coupled equations using normal coordinate corresponding to linear natural modes. The transformed equations were integrated numerically. This transformation can save computational time drastically.

In this report, the proposed method is applied to simulation for impact responses of a viscoelastic shock absorber with an elastic structure (an S-shaped structure) by colliding with a concentrated mass. The concentrated mass has initial velocities and collides with the shock absorber. Accelerations of the elastic structure and the concentrated mass are measured using Levitation Mass Method proposed by Fujii [3]. The calculated accelerations from the proposed FEM, corresponds to the experimental ones.

Moreover, using this method, we also investigate dynamic errors of the S-shaped force transducer due to elastic mode in the S-shaped structure.

Acknowledgment

This work was supported by JSPS KAKENHI Grant Number 24360156.

References

[1] T. Yamaguchi, Y. Fujii, T. Fukushima, T. Kanai, K. Nagai and S. Maruyama, "Dynamic responses for viscoelastic shock absorbers to protect a finger under impact force," *Applied Mechanics and Materials*, vol.36, pp.287-292, Oct. 2010.

[2] T. Yamaguchi, Y. Fujii, K. Nagai and S. Maruyama, "FEA for vibrated structures with non-linear concentrated spring having hysteresis," *Mechanical Systems and Signal Processing*, vol.20, pp.1905–1922, Nov. 2006.

[3] Y. Fujii, "Measurement of the electrical and mechanical responses of a force transducer against impact forces," *Review of Scientific Instruments*, vol.77, pp. 1–5, Aug. 2006.

[4] Y. Fujii and T. Yamaguchi, "Method for evaluating material viscoelasticity," *Review of Scientific Instruments*, vol.75, no.1, pp.119–123, Jan. 2004.

[5] Y. Fujii and T.Yamaguchi, "Proposal for material viscoelasticity evaluation method under impact load," *Journal of Material Science*, vol.40, no.18, pp.4785–4790, 2005.

[6] T. Yamaguchi and Y. Fujii, "Dynamic analysis by FEM for a measurement system to observe viscoelasticity using levitation mass method," *International Journal of Advanced Manufacturing and Technology*, vol.46, no.9-12, pp.885–891, 2010.